

Effect of pH on the complexation of irbesartan with β -, hydroxypropyl- β -, and γ -cyclodextrin: solubility enhancement and physicochemical characterization

Fakhri YOUSEF*

Department of Chemistry, College of Science, Al-Hussein Bin Talal University, Ma'an, Jordan

Received: 10.05.2018

Accepted/Published Online: 14.07.2018

Final Version: 06.12.2018

Abstract: The affinity of irbesartan (IRB) to form inclusion complexes with β -cyclodextrin (β -CD), hydroxypropyl- β -cyclodextrin (HP- β -CD), and γ -cyclodextrin (γ -CD) was investigated in aqueous buffered solutions at pH 1.7, 4.1, and 7.0. Analysis of the UV absorption-pH profiles revealed that IRB has two pK_a values: $pK_{a1} = 3.60$ (imidazolinone ring moiety) and $pK_{a2} = 4.70$ (tetrazole moiety). In the presence of 5.0 mmol L^{-1} β -CD, the tetrazole moiety became more acidic, indicating its inclusion within the β -CD cavity. Phase-solubility diagrams (PSDs) were obtained for IRB in aqueous buffered solutions of β -CD, HP- β -CD, and γ -CD at pH 4.1 (zwitterionic IRB), pH 1.7 (protonated IRB), and pH 7.0 (deprotonated IRB). Rigorous nonlinear regression analysis of IRB/CD PSDs at pH 4.1, where IRB is poorly soluble, yielded estimates of complex formation constants (K_{11}) that followed the decreasing order of HP- β -CD > γ -CD > β -CD. The highest solubility enhancement of IRB was achieved by complexation with HP- β -CD at pH 4.1. The formation of the IRB/ β -CD inclusion complex in solution and in the solid state has been proven through NMR, DSC, FT-IR, and XRD studies. Analysis of ^1H and ^{13}C -NMR spectra indicated the inclusion of the tetrazole-biphenyl moiety within the β -CD cavity.

Key words: Irbesartan, irbesartan-cyclodextrin complexes, irbesartan pK_a values, phase solubility analysis

1. Introduction

Irbesartan (IRB), 2-butyl-3-({4-[2-(2*H*-1,2,3,4-tetrazol-5-yl)phenyl]phenyl}methyl)-1,3-diazaspiro[4.4]non-1-en-4-one, (Figure 1) is an angiotensin II type 1 receptor (AT_1R) blocker used orally for treatment of hypertension.¹⁻⁴ Irbesartan is a class II drug according to the Biopharmaceutical Classification System, which means that it is a drug of high permeability and low aqueous solubility.⁵ The poor aqueous solubility of IRB can affect its bioavailability and therefore should be enhanced, using different solubilization techniques, in the drug formulation stage. Cyclodextrins (CDs) have been used to enhance the aqueous solubility and dissolution rate of poorly soluble drugs by partial or total encapsulation of the hydrophobic drug moieties within the hydrophobic CD cavities.⁶ Solubility enhancement of IRB by CDs has been investigated by many researchers, mostly as part of formulation studies, where IRB was complexed with β -CD and hydroxypropyl- β -CD (HP- β -CD) in the presence of many excipients and soluble polymers.⁷⁻¹⁰ However, except for the reported complexation of IRB with γ -CD at pH 7.2 and 4.3 in an eye drops preformulation study, all reported solubility enhancement investigations were performed in water without any pH control.¹¹ Accordingly, and considering that the pH of biological fluids of the human body ranges from 1.2 to 7.8, no adequate evaluation for the effect of solution pH on the solubility of IRB and its complexation with CDs was found.

*Correspondence: fakhri-yousef@ahu.edu.jo

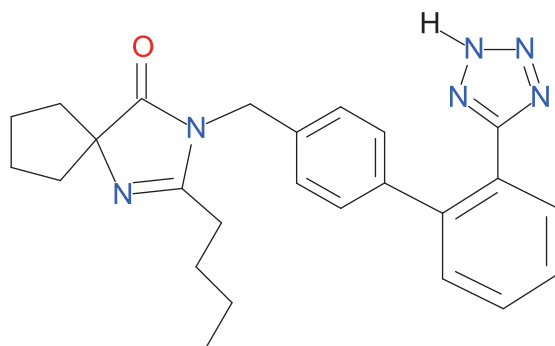


Figure 1. Structure of irbesartan.

This work investigates the solubility enhancement of IRB through complexation with β -CD, HP- β -CD, and γ -CD in aqueous 0.10 mol L^{-1} phosphate buffer solutions at pH values of 1.7, 4.1, and 7.0 through analysis of UV absorption-pH profiles, pH-solubility profiles, and phase-solubility diagrams (PSDs). In addition, and in order to confirm the formation of true inclusion complexes, the IRB/ β -CD complex is characterized in solution and in solid state. Characterization techniques include 1D NMR (^1H and ^{13}C) and 2D NMR (HMQC) spectroscopy, FT-IR spectroscopy, differential scanning calorimetry (DSC), and X-ray powder diffractometry (XRD).

It should be mentioned that the IRB/ β -CD complex was chosen for characterization because β -CD is usually the most used in industry, since it is simpler than HP- β -CD and its cavity size fits phenyl groups better than the relatively wide γ -CD cavity. Accordingly, β -CD is expected to show better interactions upon complex formation and to show more clear spectroscopic changes.

2. Results and discussion

2.1. Ionization constants ($\text{p}K_{\text{a}}$ s) of irbesartan

The change of absorbance of IRB at 243 nm at different pH values is shown in Figure 2. Analysis of the UV absorption-pH profile using Eq. (9), described in detail in the experimental section, yielded the values $\text{p}K_{\text{a}1} = 3.60$ and $\text{p}K_{\text{a}2} = 4.70$, while analysis of the pH-solubility profile (Figure 3) using Eq. (10) yielded the values $\text{p}K_{\text{a}1} = 3.62$ and $\text{p}K_{\text{a}2} = 4.91$. The discrepancy in the value of $\text{p}K_{\text{a}2}$ obtained by the UV absorption-pH profile (4.70) at fixed IRB concentration from that of the pH-solubility profile (4.91) is obviously due to the difficulty in controlling pH for the saturated solution above pH 6 in the latter method. Therefore, the $\text{p}K_{\text{a}2}$ value corresponding to the ionization of the acidic hydrogen of the tetrazole moiety obtained at $\text{p}K_{\text{a}2} = 4.70$ is more accurate. Both methods yielded a $\text{p}K_{\text{a}1}$ value of about 3.60, corresponding to the imidazolinone ring moiety. These results are in good agreement with the reported $\text{p}K_{\text{a}}$ values obtained by potentiometry and spectrofluorometry.^{12,13}

Analysis of the absorption-pH profile of IRB in the presence of 5 mmol L^{-1} β -CD yielded $\text{p}K_{\text{a}1} = 3.66$ and $\text{p}K_{\text{a}2} = 4.26$. The decrease in $\text{p}K_{\text{a}2}$ indicates that the tetrazole moiety of IRB was included within the cyclodextrin cavity upon complexation, which caused it to become more acidic. However, although the $\text{p}K_{\text{a}1}$ value of IRB did not change in the presence of β -CD, the inclusion of the imidazolinone ring moiety of IRB, partially or totally, cannot be excluded.

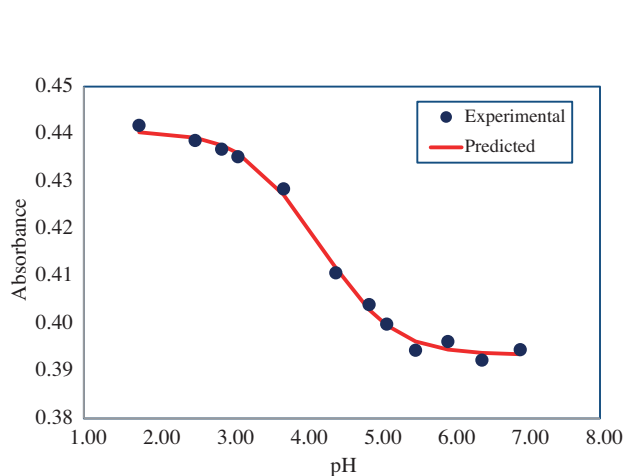


Figure 2. A plot of the variation of UV absorbance at 243 nm of $0.0025 \text{ mmol L}^{-1}$ IRB against pH of 0.10 mol L^{-1} phosphate buffer solutions at $30 \text{ }^{\circ}\text{C}$.

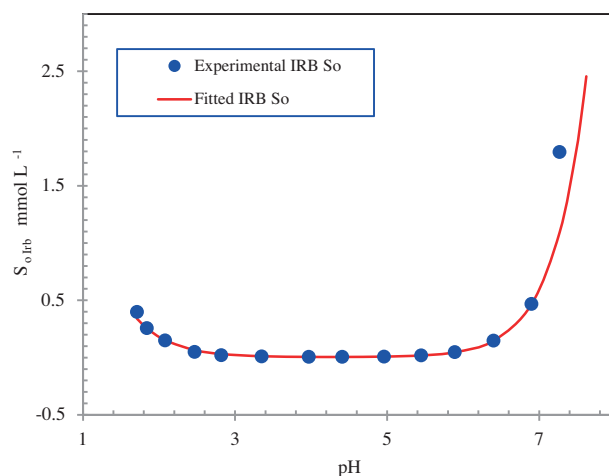


Figure 3. A plot of the variation of inherent solubility S_o of IRB against pH of 0.10 mol L^{-1} phosphate buffer solutions at $30 \text{ }^{\circ}\text{C}$.

2.2. Phase-solubility studies

The pH-solubility profile (Figure 3) shows that IRB is poorly soluble in the pH range of 1.7 to 7.0, which is similar to the pH range of the biological fluids. Accordingly, solubility enhancement of IRB by CD complexations was investigated at pH values of 1.7, 4.1, and 7.0. Figure 4 depicts the PSDs obtained for IRB against each of the β -CD, HP- β -CD, and γ -CD concentrations in aqueous 0.10 mol L^{-1} phosphate buffer at pH 4.1 and $30 \text{ }^{\circ}\text{C}$. At this pH value, IRB predominantly exists as a partly cationic and partly anionic (zwitterionic) molecule with a very low inherent solubility (S_o) of about $0.0040 \text{ mmol L}^{-1}$. Rigorous analysis of the PSDs, described in detail in the experimental section, produced estimated K_{11} values of 610, 1423, and 842 L mol^{-1} for complexation of IRB with β -CD, HP- β -CD, and γ -CD, respectively, which means that IRB forms stable 1:1 (SL-type) complexes with the three ligands. However, IRB was found to form 1:2 (SL₂-type) complexes with β -CD only (Table 1). The larger K_{11} value of HP- β -CD relative to γ -CD and β -CD can be explained in terms of the larger number of hydroxyl groups (interior and exterior of the cavity), which can facilitate more H-bonding with the zwitterionic IRB and more complex stability.^{14,15} Moreover, complexation of IRB with HP- β -CD caused the highest solubility enhancement (SE) among other cyclodextrins, where solubility enhancement is the ratio of IRB solubility in the presence of 10 mmol L^{-1} CD (S_m) to the inherent solubility in the absence of CD ($\text{SE} = S_m/S_o$). This important result indicates that, in drug formulation, HP- β -CD can be used as an efficient excipient to solubilize IRB in order to improve its dissolution profile at pH 4.1, although β -CD and γ -CD can also be used effectively as well.

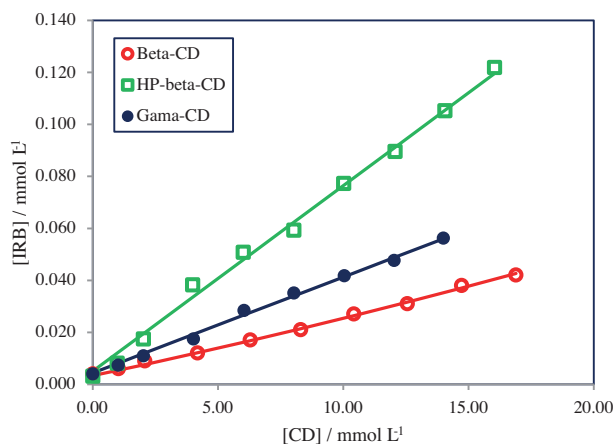
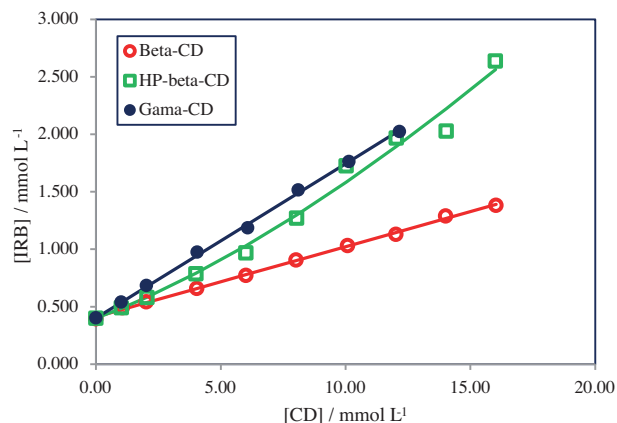
In order to investigate the mode of complexation of the protonated IRB (HIRB^+) with CDs, PSDs were obtained for IRB against β -CD, HP- β -CD, and γ -CD concentrations in 0.10 mol L^{-1} phosphate buffer at pH 1.7 and $30 \text{ }^{\circ}\text{C}$ (Figure 5). Rigorous analysis of the PSDs indicated that K_{11} values of the complexation of HIRB^+ with the three CD ligands were lower than those obtained at pH 4.1 (Table 1), with SL₂-type complexes present only with HP- β -CD. The formation of SL₂-type complexes by HP- β -CD stems from the fact that it has outer surface hydroxyl groups that can form a noninclusion complexation (through H-bonding) in addition to the inclusion complexation.¹⁴ On the other hand, the relatively larger K_{11} values observed for γ -CD at pH 1.7

Table 1. IRB/CD complexation parameters obtained from rigorous analysis of PSDs obtained in 0.10 mol L⁻¹ phosphate buffer solutions at pH 1.7, 4.1, and 7.0 at 30 °C*.

pH	CD type	K_{11} (L mol ⁻¹)	K_{12} (L mol ⁻¹)	SE
1.7	β -CD	158 \pm 11	-	2.6
	HP- β -CD	221 \pm 9	71 \pm 5	4.3
	γ -CD	386 \pm 23	-	4.4
4.1	β -CD	610 \pm 34	9 \pm 1	7.7
	HP- β -CD	1423 \pm 161	-	25.0
	γ -CD	842 \pm 65	-	10.3
7.0	β -CD	890 \pm 48	-	6.8
	HP- β -CD	940 \pm 36	-	8.4
	γ -CD	1017 \pm 81	-	9.5

* \pm Uncertainties were estimated from regression analysis for a 95% confidence level.

(and at pH 7.0 below) can be attributed to its wider cavity that can accommodate the large biphenyl-tetrazole moiety of IRB more effectively. At a pH value of 1.7, the inherent solubility (0.40 mmol L⁻¹) is much higher than that at pH 4.1 which reduces the values of the complex formation constants for all CDs. The lower K_{11} values can be attributed to the lower driving force for the inclusion of the more soluble charged HIRB⁺ species within the hydrophobic cavity of CDs. Moreover, SE values of HIRB⁺ by complexation with the three CDs were all comparable at pH 1.7, although less than those obtained for IRB at pH 4.1.

**Figure 4.** PSDs of IRB against β -CD, HP- β -CD, and γ -CD concentrations in 0.10 mol L⁻¹ phosphate buffer at pH 4.1 and 30 °C.**Figure 5.** PSDs of IRB against β -CD, HP- β -CD, and γ -CD concentrations in 0.10 mol L⁻¹ phosphate buffer at pH 1.7 and 30 °C.

Complexation of deprotonated IRB (IRB⁻) with different CDs was also investigated by obtaining PSDs for IRB against β -CD, HP- β -CD, and γ -CD concentrations in aqueous 0.10 mol L⁻¹ phosphate buffer at pH 7.0 and 30 °C (Figure 6). It was observed that, because of the much higher inherent solubility of IRB⁻ at pH 7.0 (0.54 mmol L⁻¹), it took about 5 days of shaking for the samples to reach equilibrium, especially with the more soluble CDs, HP- β -CD and γ -CD. Rigorous analysis of the PSDs revealed that IRB⁻ formed a 1:1 (SL-type) inclusion complex with β -CD with K_{11} value of 890 L mol⁻¹ within the ligand's (β -CD) solubility

range; however, IRB^- was found to form SL-type complexes with low concentrations of HP- β -CD and γ -CD only (less than 4 mmol L⁻¹). At higher concentrations of HP- β -CD and γ -CD, PSDs became more curved and the fitting conformed to predominantly SL₂-type complexes. In addition, and as can be seen in Table 1, the solubility enhancement of IRB upon complexation with β -CD and γ -CD at pH 7.0 is comparable to that at pH 4.1; however, upon complexation with HP- β -CD, the SE of IRB is much lower than that observed at pH 4.1.

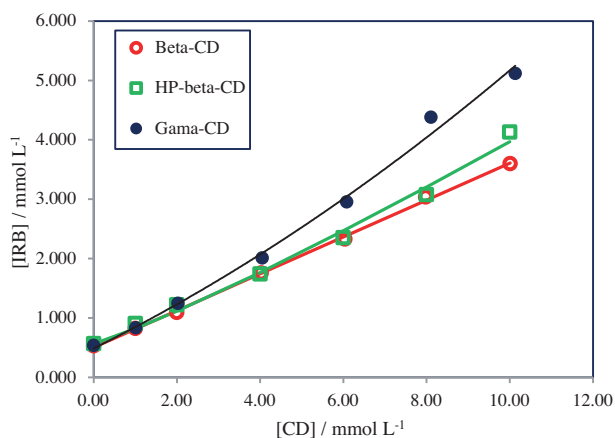


Figure 6. PSDs of IRB against β -CD, HP- β -CD, and γ -CD concentrations in 0.10 mol L⁻¹ phosphate buffer at pH 7.0 and 30 °C.

These results clearly indicate that solubility enhancement of IRB through complexation with β -CD, HP- β -CD, and γ -CD is best achieved at pH 4.1 to pH 7.0, where IRB exists as a zwitterionic or deprotonated molecule. This pronounced solubility enhancement can be attributed to more efficient complex formation in this pH range with the consequence of increased acidity of IRB due to complex formation. The formation of true IRB/CD inclusion complexes has been confirmed through characterization of the 1:1 IRB/ β -CD complex.

2.3. Characterization of the IRB/ β -CD complex

2.3.1. ¹H and ¹³C NMR spectroscopy

¹H and ¹³C NMR spectra were measured in DMSO-d₆ for β -CD, IRB, and IRB/ β -CD complexes. Comprehensive ¹H and ¹³C chemical shift assignments were made for β -CD, IRB, and IRB/ β -CD complexes and those of free IRB were found to agree with reported values.^{16,17} The formation of the IRB/ β -CD complex was proved evident from the observed proton and ¹³C chemical shift displacements ($\Delta\delta$), estimated according to $\Delta\delta = \delta_{complex} - \delta$, and from change of multiplicity of certain IRB and β -CD protons upon complexation. The penetration of the tetrazole moiety and its connected biphenyl group within the β -CD cavity was evident from the complete change of multiplicity of protons at positions 12, 13, 15, and 16 from a singlet at 7.1033 ppm to two doublets (Figure 7). Moreover, the chemical shifts corresponding to the primary hydroxyl groups situated at the narrow rim of β -CD (OH-6 triplet at 4.478 ppm) collapsed into a broad singlet at 4.4854 ppm, while those corresponding to the secondary OH-2 and OH-3 groups, situated at the wide rim of β -CD, exhibited a net chemical shift displacement of 0.013 ppm indicating an appreciable H-bonding interaction between β -CD

hydroxyl groups and the tetrazole moiety of IRB. In addition to these dramatic changes of spin multiplicity, appreciable proton chemical shift displacements were observed for the IRB aromatic rings protons at positions 19 through 22 and for H₁, H₃, H₅, and H_{6,6'} of β -CD (Table 2).

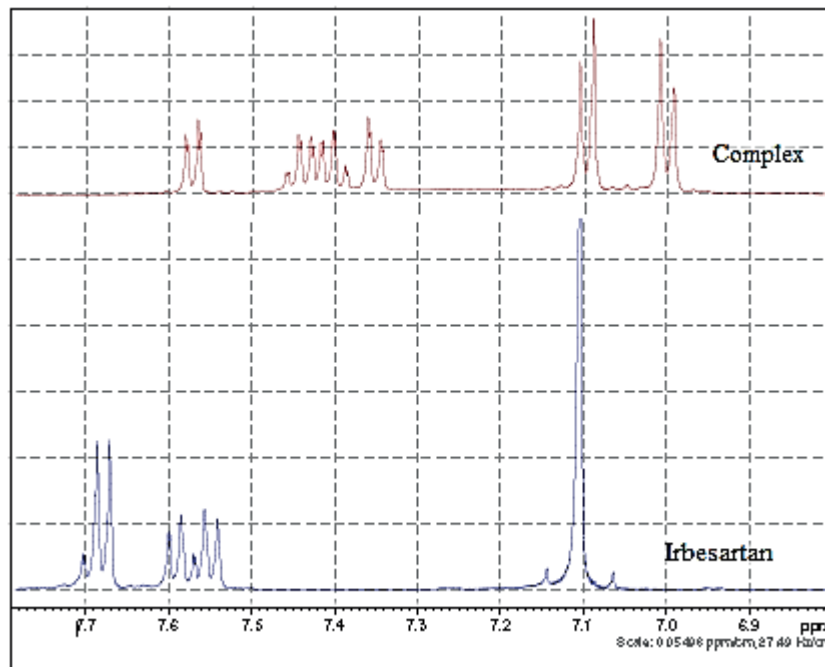


Figure 7. ¹H NMR spectra pertaining to the aromatic region of IRB, for free IRB and the corresponding IRB/ β -CD complex, obtained in DMSO-d₆ at 25 °C.

¹³C NMR spectra have shown considerable chemical shift displacements for the tetrazole and biphenyl carbons of IRB upon complexation. Inspection of Table 3 shows notably large ¹³C chemical shift displacements for the quaternary carbons at positions 11, 14, 17, and 18 of the biphenyl group and carbon 23 of the tetrazole ring (Figure 8). However, weaker ¹³C chemical shift displacements were observed for other carbons.

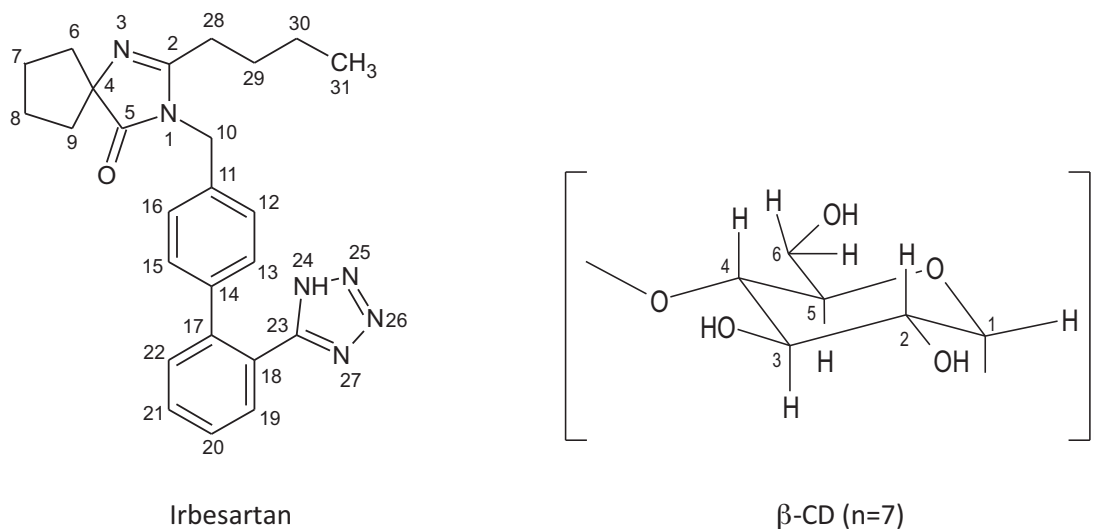
It is obvious from analysis of all ¹H and ¹³C NMR spectra that the biphenyl-tetrazole moiety of IRB is included, partially or totally, within the β -CD cavity upon complex formation.

The correlation between ¹H and ¹³C chemical shift displacements at a particular position in the complex was established through analysis of the 2D HMQC NMR spectrum (Figure 9). The coupling contours in the HMQC spectrum of the aromatic region of IRB in the complex show a clear direct C-H coupling between aromatic carbons (C12, C13, C15, and C16) and their attached split protons and aromatic carbons (C19 through C22) and their attached shifted protons, which reinforces the previous 1D NMR analysis of the complex.

2.3.2. Differential scanning calorimetry

DSC thermograms of IRB, β -CD, a 1:1 physical mixture of IRB and β -CD, and the IRB/ β -CD complex are shown in Figure 10. The DSC thermogram of IRB shows one sharp endothermic peak at about 181 °C, while that of β -CD is in the range of 30–300 °C, typical according to the reported literature.¹⁸ Figure 10 shows that while the endothermic IRB peak was still evident in the physical mixture, it disappeared completely in the thermogram of the complex, indicating the formation of IRB/ β -CD inclusion complex.

Table 2. ^1H NMR chemical shifts (δ in ppm) of free β -CD, free IRB, and IRB/ β -CD complex obtained in DMSO- d_6 at 25 $^\circ\text{C}$.



Assignment	δ	$\delta_{complex}$	$\Delta\delta_{ppm}$	
Irbesartan	22	7.5487	7.3520	-0.1967
	20	7.5837	7.4434	-0.1403
	19	7.6784	7.5719	-0.1065
	21	7.6945	7.4019	-0.2925
β -CD	H ₅	3.5663	3.5750	0.0087
	H _{6,6'}	3.6356	3.6490	0.0134
	H ₃	3.6374	3.649	0.0116
	H ₁	4.8353	4.8406	0.0053

Table 3. ^{13}C NMR chemical shifts of aromatic region carbons in free IRB and in IRB/ β -CD complex obtained in DMSO- d_6 at 25 $^\circ\text{C}$.

Position	$\delta_{irbesartan}$	$\delta_{complex}$	$\Delta\delta_{ppm}$
18	123.9636	130.6107	6.6471
12, 16	126.7492	126.0824	-0.6668
20	128.3023	127.4326	-0.8697
21	131.5495	128.5826	-2.9669
11	136.7888	135.5498	-1.2390
14	138.8483	140.9954	2.1471
17	141.4992	140.5968	-0.9024
23	155.4977	159.9962	4.4985

2.3.3. FT-IR spectroscopy

FT-IR spectra of β -CD, IRB, a 1:1 physical mixture of IRB and β -CD, and the IRB/ β -CD complex are shown in Figure 11. Inspection of the IR spectra revealed that three IR bands of IRB, which were evident in the

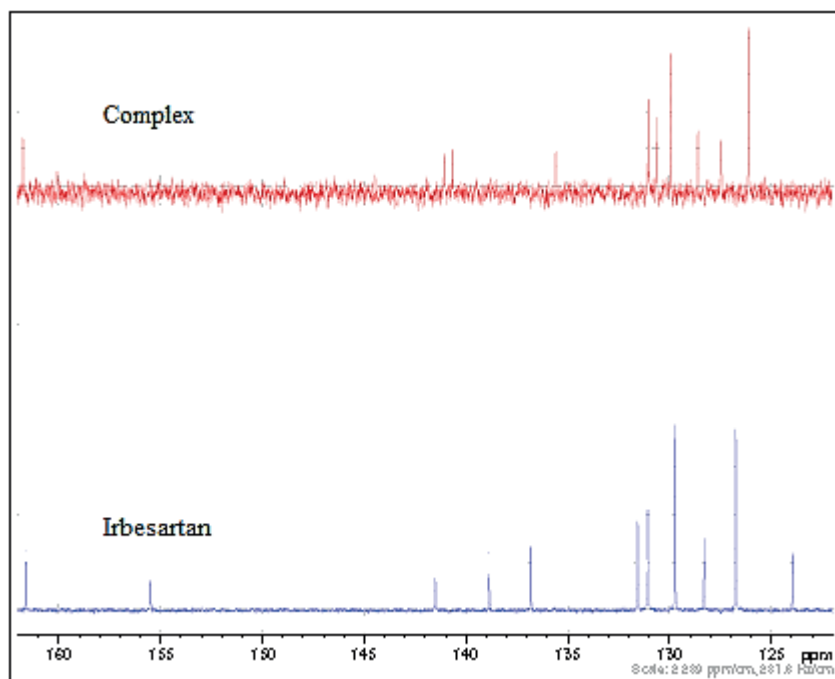


Figure 8. ^{13}C NMR spectra pertaining to the aromatic region of IRB, for free IRB and the corresponding IRB/ β -CD complex, obtained in DMSO-d_6 at 25°C .

physical mixture, appear to be shifted or attenuated upon complexation. Assignment of IR bands of IRB was made in accordance with the reported literature.¹⁹ The band at 1733 cm^{-1} assigned to the carbonyl stretching is largely attenuated, while those at 1619 cm^{-1} assigned to $\text{C2}=\text{N3}$ stretching and at 1409 cm^{-1} assigned to NNH in-plane bending were shifted to 1636 cm^{-1} and 1384 cm^{-1} , respectively. This attenuation and shifting of IR bands related to tetrazole and imidazolinone moieties indicate that IRB is included within the cyclodextrin cavity, which will induce many interactions like H-bonding with β -CD hydroxyl groups.

2.3.4. X-ray diffraction

The XRD patterns of IRB, β -CD, a 1:1 physical mixture of IRB and β -CD, and the IRB/ β -CD complex are shown in Figure 12. Inspection of the diffraction pattern of the IRB/ β -CD complex shows that most of the characteristic peaks of IRB and β -CD shown in the physical mixture are diminished, except for a few characteristic diffraction peaks that still exist: a band at $2\theta = 12^\circ$, a broad band centered at $2\theta = 20^\circ$, and two sharp peaks at $2\theta = 38^\circ$ and 44° . The reduction of crystallinity indicated by diminution of the sharp peaks of IRB and β -CD, which were still evident and overlapped in the physical mixture diffraction pattern, confirms the formation of a true IRB/ β -CD inclusion complex.

2.4. Conclusions

Irbesartan was found to have two $\text{p}K_a$ values: $\text{p}K_{a1} = 3.60$ (for imidazolinone ring moiety) and $\text{p}K_{a2} = 4.70$ (for tetrazole moiety). Irbesartan is able to form stable inclusion complexes with β -CD, HP- β -CD, and γ -CD in its protonated, zwitterionic, and deprotonated forms at pH values of 1.7, 4.1, and 7.0, respectively. As the solubility of IRB increases dramatically at pH values higher than pH 7 or lower than pH 1.7, the highest

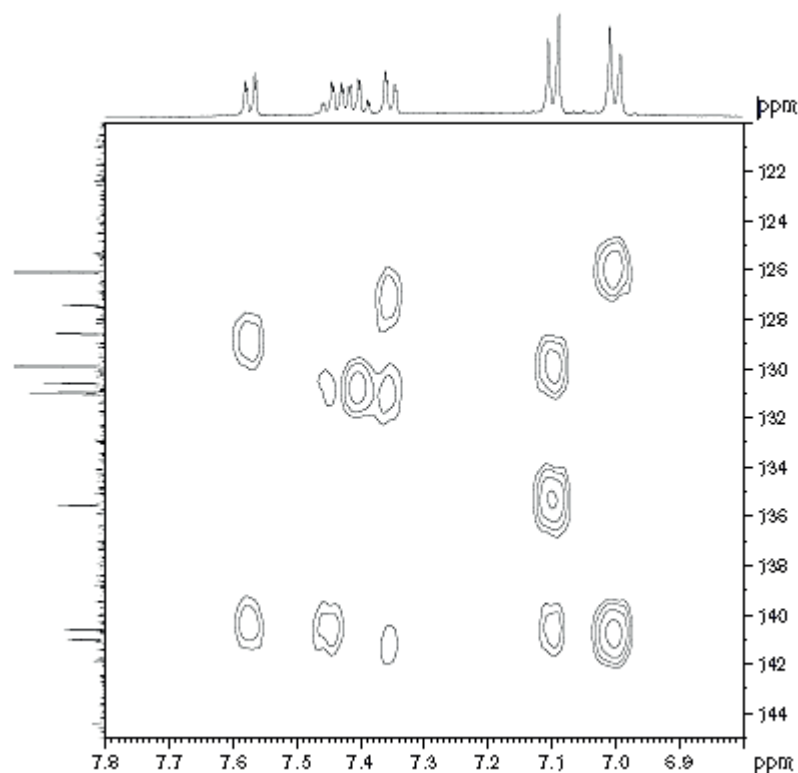


Figure 9. 2D HMQC NMR spectrum pertaining to the aromatic region of IRB in the corresponding IRB/ β -CD complex.

solubility enhancement was achieved with the poorly soluble partly neutral (zwitterionic) IRB at pH 4.1 using HP- β -CD (SE = 25); therefore, using HP- β -CD as a solubilizer in the formulation of IRB drug products is recommended. The different characterization techniques of NMR, FT-IR, DSC, and XRD confirmed the formation of a true inclusion complex of IRB with β -CD in solution and in the solid state, while ^1H and ^{13}C NMR results indicated the inclusion of the biphenyl-tetrazole moiety within the cyclodextrin cavity.

3. Experimental

3.1. Materials

Irbesartan (99.8%) was provided by Dar Al Dawa Pharmaceuticals (Jordan), β -CD (99.5%) was obtained from Acros Organics (China), γ -CD (99%) was obtained from ISP (Europe), and HP- β -CD (99.5%) was obtained from Baoji Guokang Bio-Technology (China) and all were used as received. All other chemicals were of analytical grade and water used was doubly distilled deionized water.

3.2. Methods

3.2.1. Determination of ionization constants ($\text{pK}_{\text{a}}\text{s}$) by UV absorption-pH profiles

A fixed IRB concentration of $0.0025 \text{ mmol L}^{-1}$ was prepared in aqueous 0.10 mol L^{-1} phosphate buffer solutions at pH values ranging from 1.6 to 7.0 and the absorbance was measured on a UV-Vis spectrophotometer (Varian Cary 100 Bio, Australia) at 243 nm.

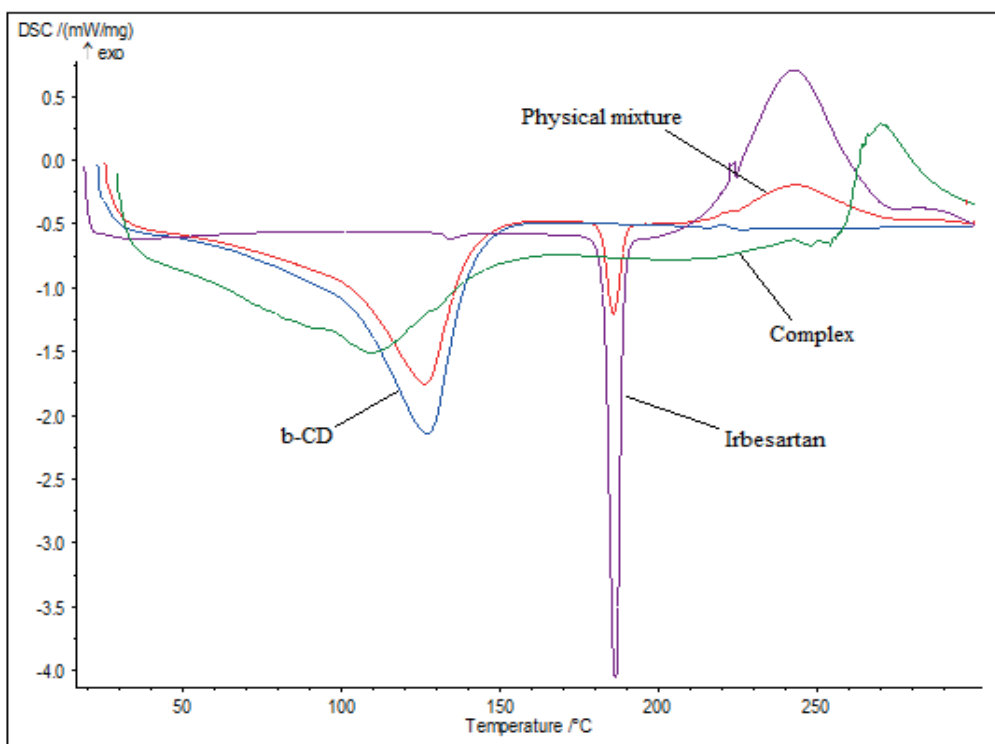


Figure 10. DSC thermograms of IRB, β -CD, a 1:1 physical mixture of IRB and β -CD, and IRB/ β -CD complex.

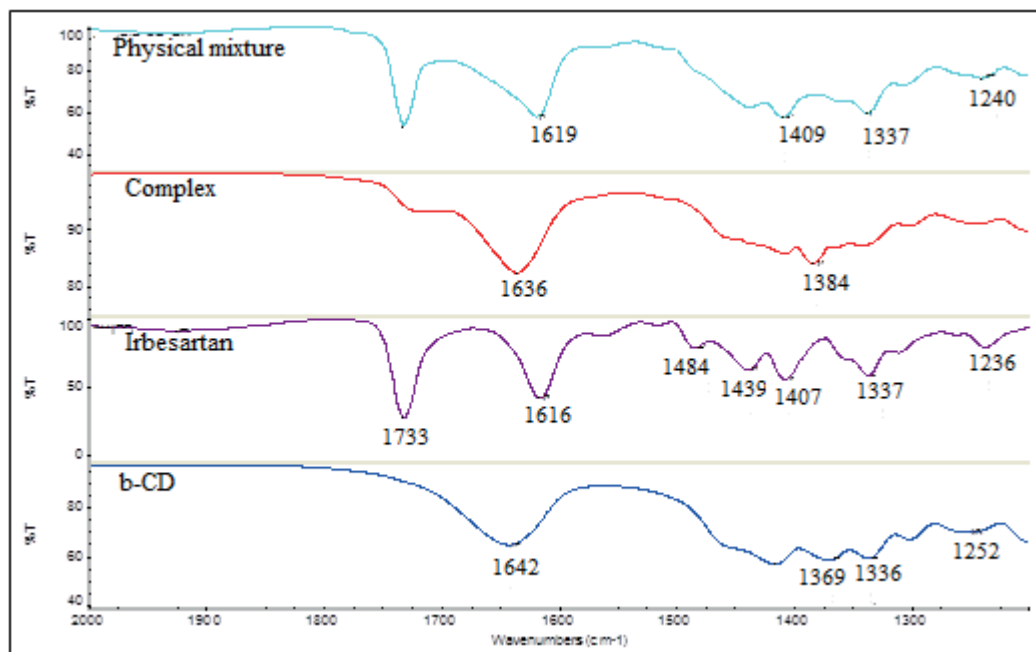


Figure 11. FT-IR spectra of IRB, β -CD, a 1:1 physical mixture of IRB and β -CD, and IRB/ β -CD complex in the spectral region of 2000–1200 cm^{-1} .

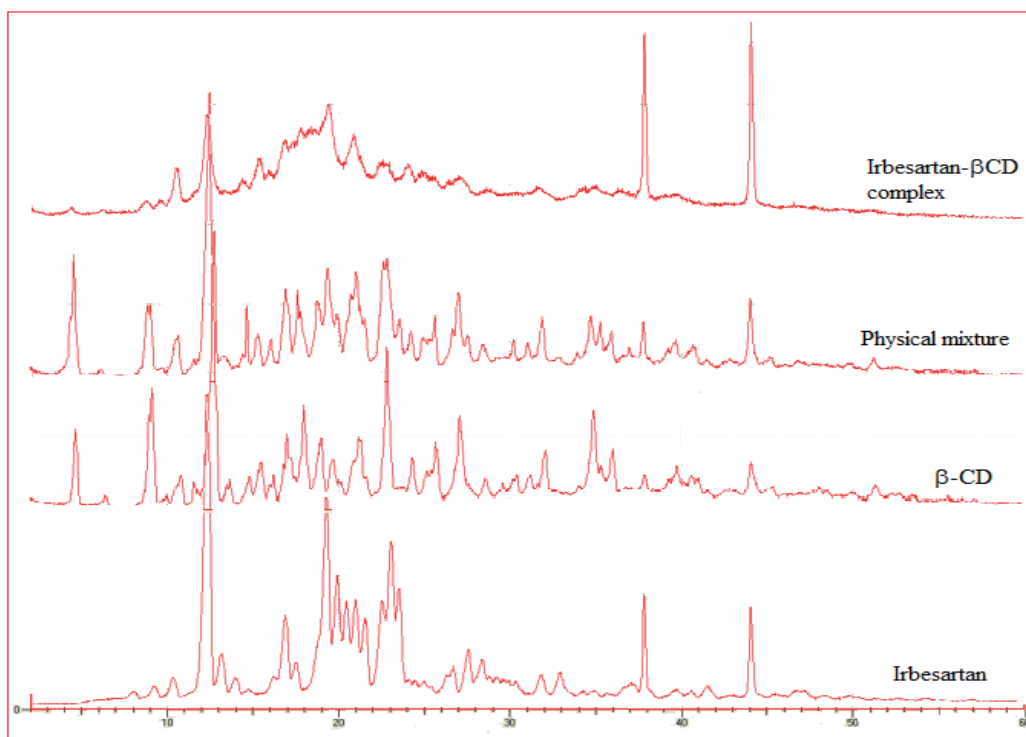
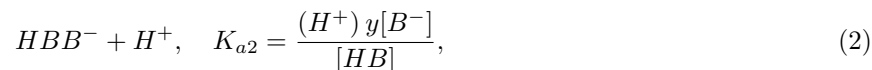
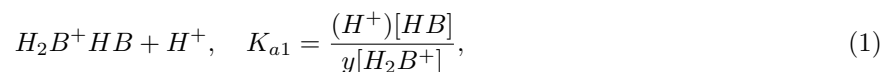


Figure 12. Powder XRD patterns of IRB, β -CD, a physical mixture of IRB and β -CD, and IRB/ β -CD complex.

In order to investigate the effect of complexation on the pK_a values, another absorption-pH profile was obtained as described above in the presence of 5.0 mmol L^{-1} β -CD. To obtain the acid/base ionization constants of IRB, which has one basic site (the imidazolinone ring moiety) and one acidic site (the acidic hydrogen of the tetrazole moiety), the measured absorbencies (A) at different pH values were analyzed through nonlinear regression as described earlier.²⁰ As IRB has one acidic site and one basic site, the equilibria involved at different pH values can be described by:



where HB, H_2B^+ , and B^- denote neutral, protonated, and deprotonated IRB, respectively. The total concentration of IRB (C) is given by:

$$C = [HB] + [H_2B^+] + [B^-], \quad (3)$$

$$C = [HB] \left\{ 1 + \frac{(H^+)}{yK_{a1}} + \frac{K_{a2}}{y(H^+)} \right\} = [HB]\alpha, \quad (4)$$

where:

$$\alpha = 1 + \frac{(H^+)}{yK_{a1}} + \frac{K_{a2}}{y(H^+)}. \quad (5)$$

(H^+) is calculated from the pH value and the activity coefficient y is given by the Davies equation:

$$\log(y) = -0.51z^2\left(\frac{\sqrt{I}}{1 + \sqrt{I}} - 0.3I\right),$$

where I is the ionic strength of the solution.

The fractions of individual IRB species (f) can be calculated by:

$$f_{HB} = \frac{C}{\alpha}, \quad (6)$$

$$f_{B^-} = \frac{\{K_{a2}/y(H^+)\}C}{\alpha}, \quad (7)$$

$$f_{H_2B^+} = \frac{\{(H^+)/yK_{a1}\}C}{\alpha}. \quad (8)$$

Combining Eqs. (3)–(8), the predicted absorbance (A^P) would be calculated by:

$$A^P = \varepsilon_{HB} f_{HB} + \varepsilon_{B^-} f_{B^-} + \varepsilon_{H_2B^+} f_{H_2B^+}, \quad (9)$$

where ε_{B^-} , ε_{HB} , and $\varepsilon_{H_2B^+}$ are the molar absorptions of B^- , HB, and H_2B^+ , respectively. Nonlinear regression of A at different pH values yields the best estimates of K_{a1} and K_{a2} by minimizing the sum of squares of errors $SSE = \sum_i (A_i^P - A_i)^2$, where A_i^P and A_i are the predicted and measured absorbance values, respectively.

In the case where 5.0 mmol L⁻¹β-CD is added to the buffer solutions, the same methodology and equations apply because α and all species fractions are a function of (H^+) and K_a values only (Eqs. (5)–(8)).

3.2.2. Analysis of pH-solubility profile

Excess amounts of IRB were added to 50.0 mL samples of aqueous 0.10 mol L⁻¹ phosphate buffer solutions having pH values of 1.7 to 7.6. The samples were mechanically shaken for 72 h at 30 °C in a thermostatic shaking water bath (GFL 1083, Germany) until equilibrium, and then an aliquot was filtered through a 0.2 μm polytetrafluoroethylene (PTFE) membrane filter (Sartorius Stedim Biotech, Germany). The IRB content was determined by measuring the spectrophotometric absorption at 243 nm and a suitable standard calibration curve.

The pH-solubility profile shows the aqueous solubility of IRB as a function of pH where it can exist in protonated, neutral, or deprotonated forms. Moreover, and based on the IRB acid/base equilibria indicated in Eqs. (1) and (2), the equilibrium solubility of IRB at different pH values is given by:

$$S_o = [HB] + [H_2B^+] + [B^-],$$

$$S_o = [HB]\left\{1 + \frac{(H^+)}{yK_{a1}} + \frac{K_{a2}}{y(H^+)}\right\}. \quad (10)$$

Best estimates for the ionization constants, K_{a1} and K_{a2} , were obtained through nonlinear regression of the experimental inherent solubility (S_o) of IRB at different pH values, which was attained by minimizing the function $SSE = \sum_i ((S_o^P)_i - (S_o)_i)^2$ where $(S_o^P)_i$ and $(S_o)_i$ are respectively the predicted and measured inherent solubility of IRB.

3.2.3. Phase-solubility diagrams

PSDs were obtained according to Higuchi and Connors, whereby excess amounts of IRB were added to 50.0 mL samples of aqueous cyclodextrin solutions with concentrations ranging from 0 to 16.0 mmol L⁻¹.²¹ All solutions were prepared in 0.10 mol L⁻¹ phosphate buffer at particular pH values (1.7, 4.1, and 7.0). The samples were mechanically shaken for 72 h at 30 °C in a thermostatic water bath until equilibrium, when an aliquot was filtered through a 0.2 µm PTFE filter and the IRB content was determined as described above. Analysis of the PSDs was performed according to an early reported rigorous procedure to obtain estimates of the IRB/CD complex formation constants.^{22,23} As a substrate (S), neutral, protonated, or deprotonated IRB may form soluble 1:1 (SL) and 1:2 (SL₂) complexes with different CD ligands (L). The equilibria involved in complex formation and the corresponding complex formation constants of SL and SL₂ complexes defined as K_{11} and K_{12} are given by:

$$S + L \rightleftharpoons SL, K_{11} = \frac{[SL]}{[S][L]},$$

$$SL + L \rightleftharpoons SL_2, K_{12} = \frac{[SL_2]}{[SL][L]}.$$

Since solutions of a given pH value are saturated with free IRB, $[S] = S_o$, the equilibrium solubilities of IRB (S_{eq}) and of CD (L_{eq}) are given by:

$$\begin{aligned} S_{eq} &= [S] + [SL] + [SL_2] \\ &= S_o + K_{11}S_o[L] + K_{11}K_{12}S_o[L]^2, \end{aligned} \quad (11)$$

$$\begin{aligned} L_{eq} &= [L] + [SL] + 2[SL_2] \\ &= [L] + K_{11}S_o[L] + 2K_{11}K_{12}S_o[L]^2, \end{aligned} \quad (12)$$

where $[L]$ denotes the concentration of free CD and $[SL]$ and $[SL_2]$ represent the concentrations of 1:1 and 1:2 IRB/CD complexes, respectively.

Therefore, the value of free CD $[L]$ was estimated by:

$$[L] = \frac{-b + \sqrt{b^2 - 4aL_{eq}}}{2a}, \quad (13)$$

where $a = 2K_{11}K_{12}S_o$ and $b = 1 + K_{11}S_o$.

Best estimates of S_o , K_{11} , and K_{12} were obtained for each phase diagram by minimizing the function $SSE = \sum_i ((S_{eq}^p)_i - (S_{eq})_i)^2$, where $(S_{eq}^p)_i$ and $(S_{eq})_i$ are respectively the predicted and measured equilibrium solubility of IRB at different CD concentrations.

3.3. Preparation of the IRB/ β -CD inclusion complex

Using a procedure similar to that described earlier, an IRB/ β -CD solid physical mixture was prepared in a 1:1 stoichiometric molar ratio.²⁴ Then 1.0 g of the solid mixture was dissolved in 100 mL of 0.005 mol L⁻¹ ammonia solution and shaken for 24 h at room temperature to assure complete dissolution; the solution was then freeze-dried in a freeze-drying apparatus (Heto Power Dry PL9000, Denmark).

3.4. Nuclear magnetic resonance spectroscopy (NMR)

^1H and ^{13}C NMR spectra of IRB, β -CD, and IRB/ β -CD complexes were obtained at 25 °C in DMSO- d_6 on a Bruker 500 MHz Avance III spectrometer. The position of the DMSO- d_6 solvent line at 2.5 ppm was used as a reference in all measurements.

3.5. Differential scanning calorimetry

Thermal behaviors of freeze-dried IRB, β -CD, a 1:1 (molar ratio) physical mixture of IRB and β -CD, and the IRB/ β -CD complex were examined using a differential scanning calorimeter (A NETZSCH 204 F1 Phoenix, Germany). An accurately weighed sample of each solid (ca. 1–3 mg) was heated in a sealed aluminum pan under nitrogen, using an empty pan sealed as a reference, over the temperature range from 30 to 300 °C at a rate of 10 °C/min.

3.6. Fourier transform infrared spectroscopy

The IR spectra of freeze-dried IRB, β -CD, a 1:1 (molar ratio) physical mixture of IRB and β -CD, and the IRB/ β -CD complex were recorded at room temperature as an average of 32 scans at a resolution of 4.0 cm^{-1} using an FT-IR spectrometer (model 670 NEXUS, Thermo Nicolet, USA) in the 400–4000 cm^{-1} range.

3.7. X-ray powder diffractometry

The XRD patterns were measured for samples of freeze-dried IRB, β -CD, a 1:1 (molar ratio) physical mixture of IRB and β -CD, and the IRB/ β -CD complex with an XRD-7000 X-ray diffractometer (Shimadzu, Japan). Radiation generated from a Cu X-ray tube with a wavelength of 1.54 Å at 30 mA and 40 kV was used. The instrument operated over the 2θ range of 2° to 60°.

Acknowledgments

I would like to thank Dar Al Dawa Pharmaceuticals for providing the irbesartan sample as a gift and the Jordanian Pharmaceutical Manufacturing Company (JPM) for performing the freeze-drying of samples. I am also grateful to Professor MB Zughul for his technical assistance and to Fatima Mustapha and Ruba Zalloum from the University of Jordan for conducting the NMR, FT-IR, and DSC studies.

References

1. Wu, J.; Ding, W.; Zhao, J.; Zang, W.; Matsuura, H.; Horie, M. *J. Renin Angiotensin Aldosterone Syst.* **2013**, *15*, 341-347.
2. Vanderheyden, P.; Verheijen, I.; Fierens, F.; De Backer, J.; Vauquelin, G. *J. Renin Angiotensin Aldosterone Syst.* **2000**, *1*, 159-165.
3. Weber, M. A. *J. Renin Angiotensin Aldosterone Syst.* **2003**, *4*, 62-73.
4. Brunetti, N. D.; De Gennaro, L.; Pellegrino, P. L.; Cuculo, A.; Ziccardi, L.; Gaglione, A.; Di Biase, M. *Eur. J. Cardiovasc. Prev. Rehabil.* **2011**, *18*, 424-437.
5. Ranjita, S. *J. Pharm. Investig.* **2013**, *43*, 1-26.
6. Takahashi, A. I.; Veiga, F. J. B.; Ferraz, H. G. *Int. J. Pharm. Sci. Rev. Res.* **2012**, *12*, 1-7.
7. Earle, R. R.; Tedlapu, V. K.; Ayalasangamajula, L. U. *Res. J. Pharm. Technol.* **2017**, *10*, 301-306.

8. Hirlekar, R.; Kadam, V. *AAPS PharmSciTech* **2009**, *10*, 276-281.
9. Kane, R.; Naik, S.; Bumrela, S.; Kuchekar, B. *J. Pharm. Res.* **2009**, *2*, 1359-1364.
10. Hirlekar, R. S.; Sonawane, S. N.; Kadam, V. J. *AAPS PharmSciTech* **2009**, *10*, 858-863.
11. Muankaew, C.; Jansook, P.; Stefansson, E.; Loftsson, T. *Int. J. Pharm.* **2014**, *474*, 80-90.
12. Tosco, P.; Rolando, B.; Fruttero, R.; Henchoz, Y.; Martel, S.; Carrupt, P.; Gasco, A. *Helv. Chim. Acta* **2008**, *91*, 468-482.
13. Cagigal, E.; Gonzalez, L.; Alonso, R. M.; Jimenez, R. M. *J. Pharm. Biomed. Anal.* **2001**, *26*, 477-486.
14. Brewster, M. E.; Loftsson, T. *Adv. Drug Deliv. Rev.* **2007**, *59*, 645-666.
15. Liu, L.; Guo, Q. X. *J. Incl. Phenom. Macrocycl. Chem.* **2002**, *42*, 1-14.
16. Bauer, M.; Harris, R. K.; Rao, R. C.; Apperley, D. C.; Rodger, C. A. *J. Chem. Soc. Perkin Trans.* **1998**, *2*, 475-481.
17. Byard, S. J.; Herbert, J. M. *Tetrahedron* **1999**, *55*, 5931-5936.
18. Bettinetti, G.; Novák, C.; Sorrenti, M. *J. Therm. Anal. Calorim.* **2002**, *68*, 517-529.
19. Franca, C. A.; Etcheverry, S. B.; Diez, R. P.; Williams, P. A. M. *J. Raman Spectrosc.* **2009**, *40*, 1296-1300.
20. Al Omari, M. M.; Zughul, M. B.; Davies, J. E. D.; Badwan, A. A. *J. Pharm. Biomed. Anal.* **2006**, *41*, 857-865.
21. Higuchi, T.; Connors, A. In *Advances in Analytical Chemistry and Instrumentation Vol. 4*; Reilley, C. N., Ed. Interscience Publishers: Hoboken, NJ, USA, 1964, pp. 117-211.
22. Zughul, M. B.; Badwan, A. A. *J. Incl. Phenom. Mol. Recognit. Chem.* **1998**, *31*, 243-264.
23. Zughul, M. B. *J. Incl. Phenom. Macrocycl. Chem.* **2007**, *57*, 525-530.
24. Cappello, B.; Maio, C.; Iervolino, M.; Miro, A. *J. Incl. Phenom. Macrocycl. Chem.* **2006**, *54*, 289-294.